

RESEARCH PAPER

## Green Synthesis of Iron Oxide-Palladium Nanocomposites by Pepper extract and Its Application in Removing of Colored Pollutants from Water

Shahab Khaghani <sup>1,\*</sup>, Davood Ghanbari <sup>2</sup>, Shohreh Khaghani <sup>1</sup>

<sup>1</sup> Young Researchers and Elite Club, Arak Branch, Islamic Azad University, Arak, Iran

<sup>2</sup> Department of Science, Arak University of Technology, Arak, Iran

### ARTICLE INFO

#### Article History:

Received 06 May 2017

Accepted 2 June 2017

Published 01 July 2017

#### Keywords:

Dendrite

Nanocomposite

Nanoparticles

Photo-catalyst

### ABSTRACT

Fe<sub>3</sub>O<sub>4</sub> nanoparticles were synthesized in the presence of pepper extract as a capping agent via a hydrothermal method. Then palladium nanoparticles and Fe<sub>3</sub>O<sub>4</sub>-Pd nanocomposites were synthesized with the aid of pepper extract as a reducing agent. Vibrating Sample magnetometer illustrated that Fe<sub>3</sub>O<sub>4</sub> nanoparticles have super paramagnetic behaviour. The photo catalytic behaviour of Fe<sub>3</sub>O<sub>4</sub>-Pd nanocomposites was investigated using the degradation of two azo dyes under ultraviolet light irradiation. The results show that nanocomposites have feasible magnetic and photo catalytic properties. The prepared products were characterized by X-ray diffraction pattern, scanning electron microscopy, transmission electron microscopy and Fourier transform infrared spectroscopy.

#### How to cite this article

Khaghani S, Ghanbari D, Khaghani S. Green Synthesis of Iron Oxide-Palladium Nanocomposites by Pepper extract and Its Application in Removing of Colored Pollutants from Water. J Nanostruct, 2017; 7(3):175-182. DOI: 10.22052/jns.2017.03.002

### INTRODUCTION

About fifty percent of the applied of palladium is used in catalytic performances like Lindlar catalyst and Suzuki coupling, which can transform around ninety percent of the noxious gases (hydrocarbons and nitrogen dioxide) into less harmful compounds (nitrogen, carbon dioxide and water vapor). Palladium is also used in dentistry, medicine, cold fusion, fuel cells, hydrogen purification, groundwater treatment, jewelry, blood sugar test strips, aircraft spark plugs, surgical instruments, breaking of carbon-carbon bonds, organo-metallic compounds, homogenous catalyst and electrical contacts. When the ratio of surface compare to volume is increased like dispersion of palladium on the carbon, various effective catalysts were prepared which it catalysis hydrogenation, dehydrogenation, and petroleum cracking [1-6]. As is clear solvo-thermal (hydrothermal) is one of the unique chemical procedures for preparation

of nanostructures with preferential and controlled shape and dimensions. While the main morphology in other methods like sol-gel and sonochemical is zero dimensional nanoparticles. Usually by hydrothermal method we can achieve preferential growth in comparison to spherical nucleation. In hydrothermal method because of high temperature and pressure the nanoparticles grow in situ and form hierarchical structures [7-9]. Magnetic separation is considered as a high speed and effective technique for separating magnetic particles. Thus, if the photocatalyst is magnetic, it could be gathered conveniently by magnetic field. Hydrothermal synthesis can be defined as a method of synthesis of single crystals that depends on the solubility of minerals in hot water under high pressure.

The free electron gas of noble metal nanoparticles features a resonant oscillation during illumination in the visible part of the

\* Corresponding Author Email: sh-khaghani@iau-arak.ac.ir

spectrum. The spectral properties of this resonance related to the material, size and dimension. Localized surface plasmon (LSP) are accompanied by valuable physical effects such as optical near-field enhancement, heat generation and excitation of hot-electrons. Also, plasmonic nanoparticles can be as efficient nano-sources of heat, light or energetic electrons, remotely controllable by light [10-17]. The photo catalytic behaviour of  $\text{Fe}_3\text{O}_4$ -Pd nanocomposites was evaluated using the degradation of two various azo dyes under ultraviolet light irradiation. The results show that nanocomposites have applicable super paramagnetic and photo catalytic performance.

#### MATERIALS AND METHODS

$\text{Fe}(\text{NO}_3)_3 \cdot 9\text{H}_2\text{O}$ ,  $\text{FeCl}_2 \cdot 4\text{H}_2\text{O}$ ,  $\text{K}_2\text{PdCl}_4$ ,  $\text{NaBH}_4$ , ammonia and distilled water were purchased from Merck Company was prepared. Scanning electron microscopy images were obtained using a LEO instrument model 1455VP. All the chemicals were used as received without further purifications. Before to taking images, the samples were coated by a very thin layer of Au (using a BAL-TEC SCD 005 sputter coater) to make the sample surface conductor and prevent charge accumulation, and obtaining a better contrast. X-ray diffraction patterns were recorded by a Philips, X-ray diffractometer using Ni-filtered



Fig. 1. Schematic of nanocomposite preparation.

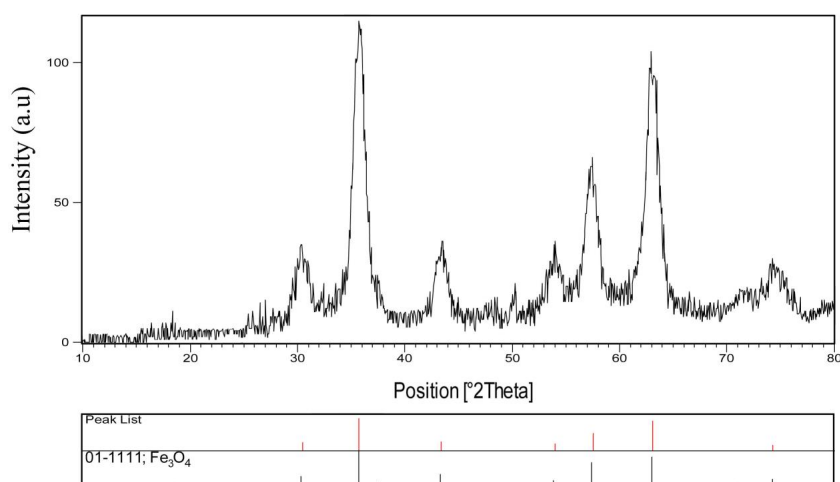


Fig. 2. XRD pattern of  $\text{Fe}_3\text{O}_4$  nanoparticles.

CuK $\alpha$  radiation. Room temperature magnetic properties were investigated using a vibrating sample magnetometer (VSM) device, (Meghnatis Kavir Khashan Co., Iran) in an applied magnetic field sweeping between  $\pm 11000$  Oe.

#### Preparation of $Fe_3O_4$ nanoparticles

0.001 mol of  $FeCl_2 \cdot 4H_2O$  and 0.002 mol of  $Fe(NO_3)_3 \cdot 9H_2O$  were dissolved in 200 mL of distilled water. Then 10 ml of pepper extract as surfactant was added to the solution, it was mixed on magnetic stirring for 10 min. 10ml of  $NH_3$  (8M) as precipitator was slowly added to reaching pH of solution to 10. The solution is put into an autoclave and oven at  $160^\circ C$  for 4 hours. The obtained black precipitate was washed twice with distilled water. Then it was dried in oven for 24h .

#### Preparation of Pd and $Fe_3O_4$ -Pd nanocomposites

0.2g of  $K_2PdCl_4$  was then dissolved in the solution (a piece of pure silver is necessary for preparation of dendrite structures) . Then 10 ml of pepper extract as reducing agent was added to the solution and was mixed for 2h. The solution is put into an autoclave and oven at  $160^\circ C$  for 4 hours.

For preparation of nanocomposite all procedures were performed at the same form just in the presence of magnetite core, firstly 0.1 g of synthesized magnetite nanoparticles was dispersed in 200 ml of distilled water and then 0.2g of  $K_2PdCl_4$  was then dissolved in the solution (a piece of pure silver is necessary for preparation of dendrite structures) . Then 10 ml of pepper extract as reducing agent was added to the solution and was mixed for 2h. The solution is put into an autoclave and oven at  $160^\circ C$  for 4 hours. (Fig..1).

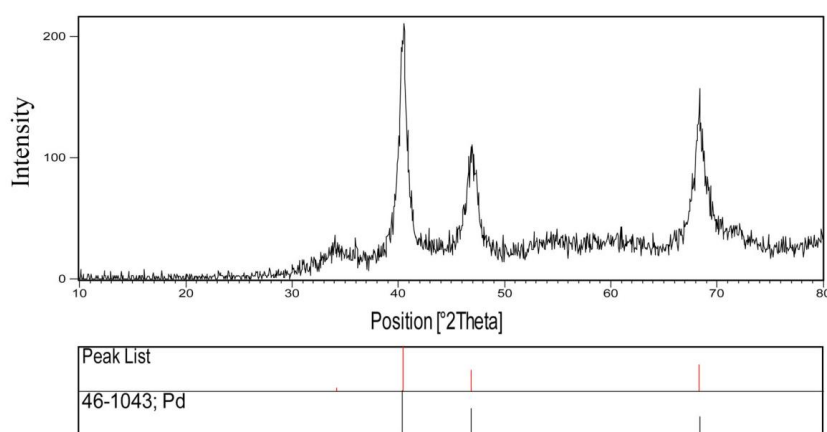


Fig. 3. XRD pattern of Pd nanoparticles.

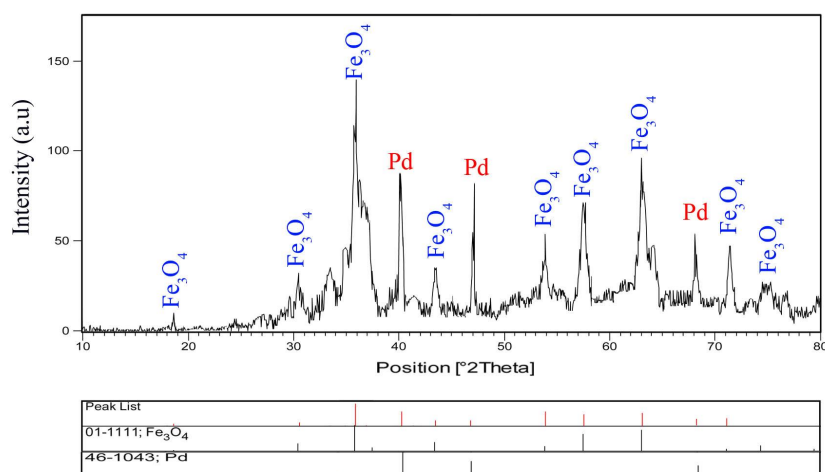


Fig. 4. XRD pattern of  $Fe_3O_4$ -Pd nanocomposite.

#### Photo-catalyst investigation

0.1 g of catalyst was applied for degradation of 10 ml (20ppm) solution. The solution was mixed by a magnet stirrer for 1 hour in darkness to determine the adsorption of the dye by catalyst and better availability of the surface. The solution was irradiated by five (8 W) UV lamp which was placed in a quartz pipe in the middle of reactor. The samples were filtered, centrifuged and their concentration was determined by UV-Visible spectrometry.

#### RESULTS AND DISCUSSION

Fig. 2 illustrates XRD pattern of magnetite. It can be observed that cubic phase (JCPDS No.01-1111) with Fd-3m space group which is consistent with pure magnetite was prepared. Fig. 3 shows XRD pattern of pure cubic palladium product (JCPDS No:46-1043, space group: Fm-3m). Fig. 4 shows XRD pattern of magnetite-palladium product. Pattern confirms presence of both nano-sphere magnetites with dendrite like palladium nanostructures. A number of strong

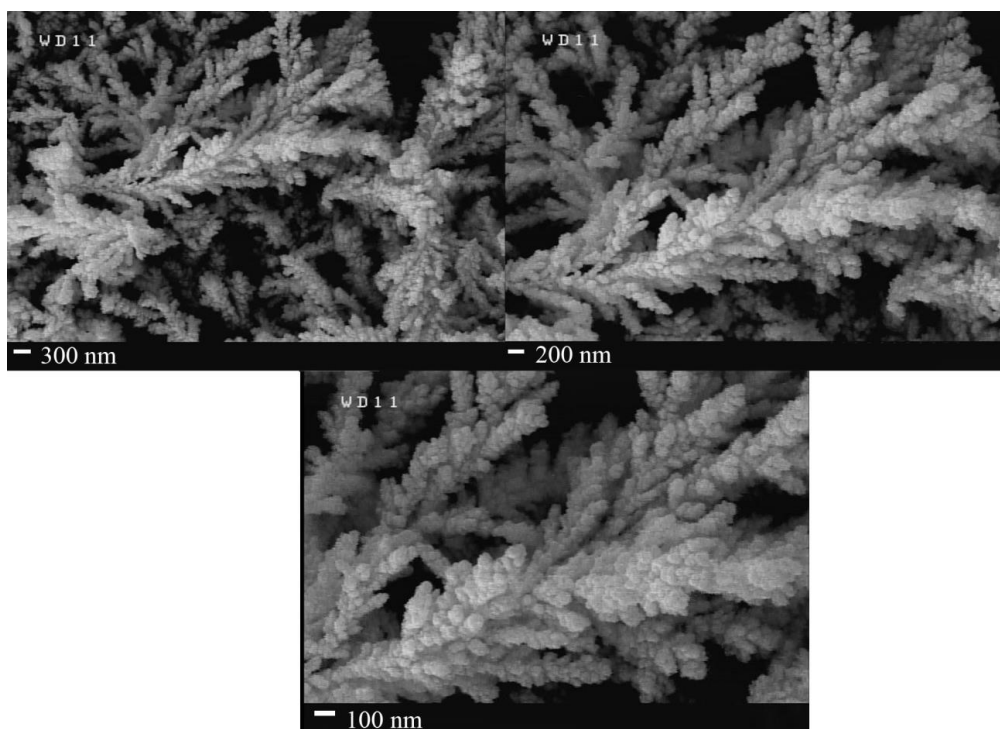


Fig. 5. SEM images of Pd dendrite nanostructures.



Fig. 6. TEM image of Pd dendrite nanostructures.

Bragg reflection peaks can be seen which of FCC palladium and lattice parameters of  $a = b = c = 3.8902 \text{ \AA}$ . The standards (JCPDS), palladium file No. 04-0783 and space group of Fm-3m (space group number: 225) in the pattern are reported. The calculated crystalline sizes from Scherrer equation,  $D_c = K\lambda/\beta\cos\theta$ , where  $\beta$  is the width of the observed diffraction peak at its half maximum intensity (FWHM),  $K$  is the shape factor, which takes a value of about 0.9, and  $\lambda$  is the X-ray wavelength ( $CuK_\alpha$  radiation, equals to 0.154 nm) were about 33 and 43 nm for  $Fe_3O_4$  and Pd nanoparticles, respectively

SEM images of the synthesized palladium nanostructures with 10 ml of pepper extract as

reducing and precipitation agent are shown in Fig. 5. Results confirm dendrite like nanostructures with average diameter size less than 100 nm were prepared.

Fig. 6 illustrates TEM image of the synthesized Pd nanoparticles with 10 ml of pepper extract by hydrothermal reaction at  $160 \text{ }^\circ\text{C}$  for 4h. Results confirm flower like nanostructures were prepared and nanoparticles with average diameter size less than 90 nm were obtained.

It is known that the particle size and shape can be controlled by modifying the super-saturation during the nucleation and crystal growth in hydrothermal, which in turn, it can strongly be

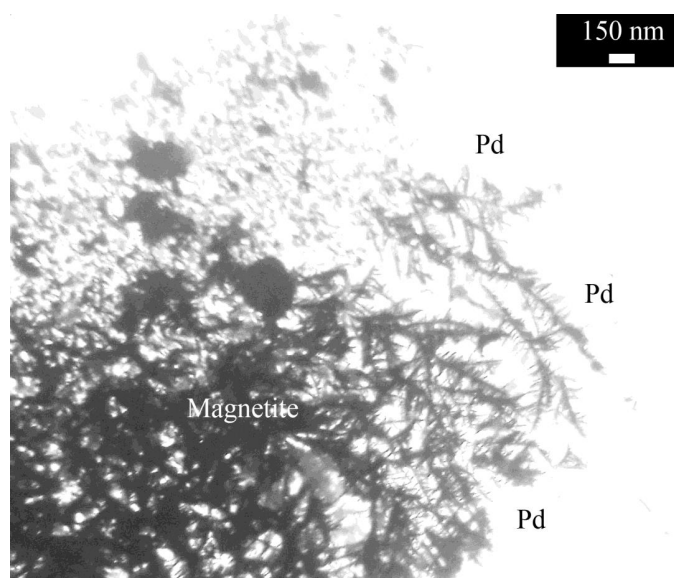


Fig. 7. TEM image of  $Fe_3O_4$ -Pd nanocomposite.

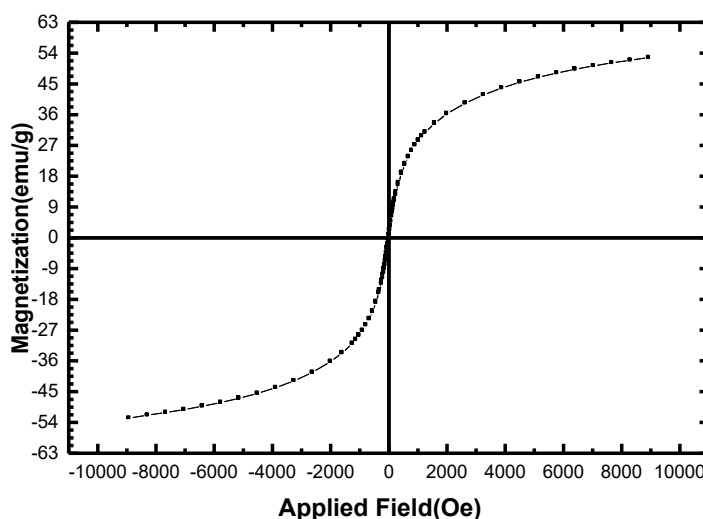


Fig. 8. Room temperature hysteresis loop of  $Fe_3O_4$  nanoparticles.

affected by solution chemistry of hydrothermal conditions such as temperature, precursor and time a of process environment.

Fig. 7 shows TEM image of  $\text{Fe}_3\text{O}_4$ -Pd nanocomposite at 160 °C for 4h. Images approve presence of both nano-sphere magnetites beside dendrite like palladium nanostructures with average particle size around 50 nm. The balance between nucleation rate and growth rate which determines final particle size and morphology

Magnetic properties of samples were studied using vibrating sample magnetometer system at room temperature. Hysteresis loop of magnetic  $\text{Fe}_3\text{O}_4$  nanoparticles at 160°C by 10 ml of pepper extract is shown in Fig. 8. Nanoparticles show super paramagnetic behaviour and have a saturation

magnetization of 56 emu/g and a coercivity tending to zero Oe. It shows a sufficient magnetization of these nanoparticles for being recycled by a magnet, making them appropriate for core of recyclable photo-catalyst. As-synthesized  $\text{Fe}_3\text{O}_4$ -Pd 10% nanoparticles show super paramagnetic behaviour and have a saturation magnetization of 46 emu/g and a coercivity about zero Oe (Fig. 9).

Hysteresis loop of magnetic  $\text{Fe}_3\text{O}_4$ -Pd 50%:50% nanoparticles prepared by simple hydrothermal is depicted in Fig. 10. The product also illustrates super paramagnetic behaviour and has a saturation magnetization of 25 emu/g and a coercivity tending to zero Oe.

This magnetization indicates that  $\text{Fe}_3\text{O}_4$ -Pd nanocomposites inherit the magnetic property

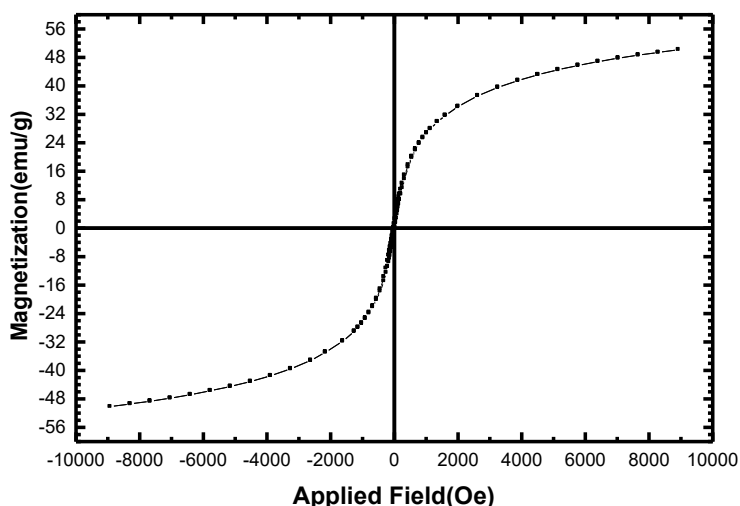


Fig. 9. VSM curve of  $\text{Fe}_3\text{O}_4$ -Pd 90%:10% nanocomposites.

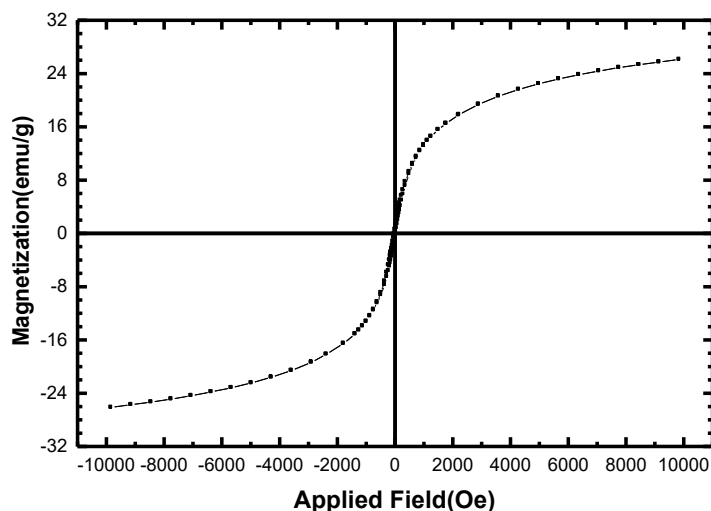


Fig. 10. Hysteresis curve of  $\text{Fe}_3\text{O}_4$ -Pd 50%:50% nanocomposite.

from the  $\text{Fe}_3\text{O}_4$ ; however, the magnetization is lower due to presence of palladium. The magnetic property of the prepared nanocomposites is an essential characteristic of a reusable magnetic heterogeneous catalyst.

The photo-catalytic activity of the  $\text{Fe}_3\text{O}_4$ -Pd nanocomposite was investigated by measuring the decomposition of Acid-Brown and Acid Black

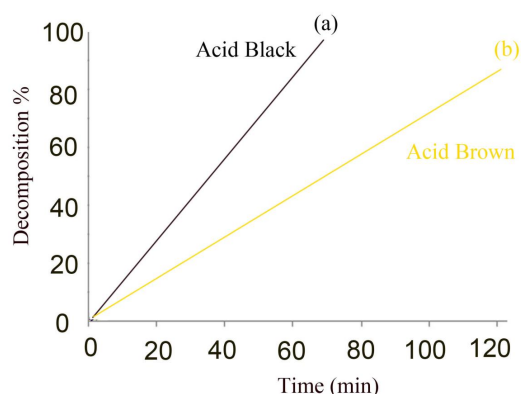


Fig. 11. Photo degradation of (a) Acid Black (b) Acid Brown.

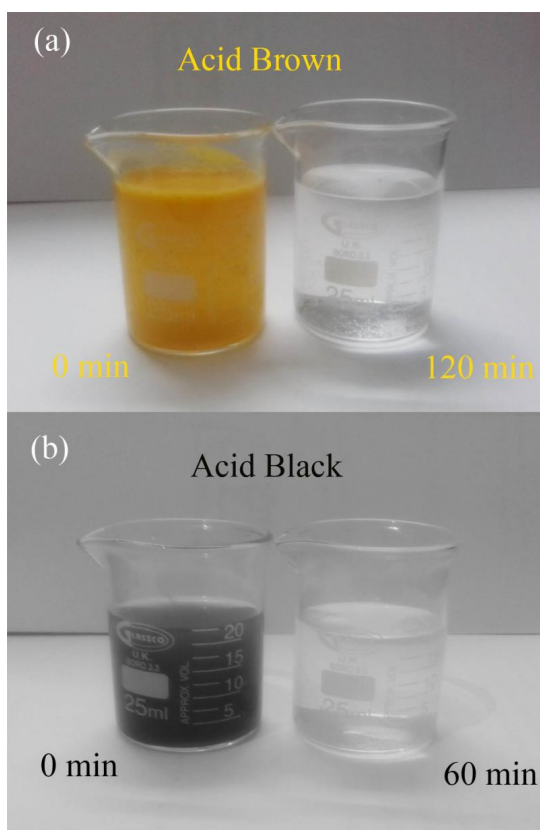


Fig. 12. Photo degradation of (a) Acid Brown (b) Acid Black

in an aqueous solution, under irradiation with UV light. The changes in the intensity of maximum wave length of two azo-dyes are depicted in Fig. 11. Maximum wave length of Acid Black and Acid-Brown were degraded about 97% and 85% in 120 min in the presence of magnetite-palladium. Acid black showed the fastest decomposition at 60 min under ultraviolet light and at presence of magnetic photo-catalyst. Organic dyes decompose to carbon dioxide, water and other less noxious or nontoxic residuals [14-17]. Fig. 12 shows degradation of the two azo dyes after 120 min exposure to the  $\text{Fe}_3\text{O}_4$ -Pd nanocomposite.

## CONCLUSIONS

Magnetite nanoparticles were synthesized via a hydrothermal in the presence of pepper extract, and then palladium nanoparticles and  $\text{Fe}_3\text{O}_4$ -Pd nanocomposites were prepared by hydrothermal method. Effects of various concentration of pepper extract were investigated on the morphology and particle size of the products. Vibrating sample magnetometer confirmed that nanocomposites exhibit super-paramagnetic behaviour. The photocatalytic behaviour of  $\text{Fe}_3\text{O}_4$ -Pd nanocomposite was evaluated using the degradation of two azo dyes under UV-visible light irradiation. The results show that pepper extract is suitable method for preparation of  $\text{Fe}_3\text{O}_4$ -Pd nanocomposites as a candidate for photocatalytic applications.

## CONFLICT OF INTEREST

The authors declare that there are no conflicts of interest regarding the publication of this manuscript.

## REFERENCES

- Chen, W. (2002). "Synthesis and Structure of Formally Hexavalent Palladium Complexes". *Science*. 295 (5553): 308.
- Crabtree, R. H. (2002). "Chemistry: A New Oxidation State for Pd?". *Science*. 295 (5553): 288.
- Powers, D. C.; Ritter, T. (2011). "Palladium(III) in Synthesis and Catalysis" (PDF). *Top. Organomet. Chem. Topics in Organometallic Chemistry*. 35: 129–156.
- Yin, Xi; Warren, Steven A.; Pan, Yung-Tin; Tsao, Kai-Chieh; et al. (2014). "A Motif for Infinite Metal Atom Wires". *Angewandte Chemie International Edition*. 53 (51): 14087–14091
- Crabtree, Robert H. (2009). "Application to Organic Synthesis". *The Organometallic Chemistry of the Transition Metals*. John Wiley and Sons. p. 392. ISBN 978-0-470-25762-3.
- Hammond, C. R. (2004). "The Elements". *Handbook of Chemistry and Physics (81st ed.)*. CRC press. ISBN 0-8493-0485-7.

7. Nabiyouni G, Ghanbari D, Fe-Ag nanocomposite: Hydrothermal preparation of iron nanoparticles and silver dendrite like nanostructures. *J Nanostruct.* 2017; 7 (2): 11-120.
8. Asiabani N, Nabiyouni G, Khaghani S, Ghanbari D, Green synthesis of magnetic and photo-catalyst  $PbFe_{12}O_{19}$ -PbS nanocomposites by lemon extract: nano-sphere  $PbFe_{12}O_{19}$  and star-like PbS. *J. Mater. Sci. Mater. Electron*, 2017;28: 1101-1114
9. Khaghani S, Ghanbari D, Magnetic and photo-catalyst  $Fe_3O_4$ -Ag nanocomposite: green preparation of silver and magnetite nanoparticles by garlic extract. *J. Mater. Sci. Mater. Electron*, 2017; 28 2877-2886:
10. Jalajjerdi R, Ghanbari D, Microwave Synthesis and Magnetic Investigation of  $CuFe_2O_4$  Nanoparticles and Poly Styrene-Carbon Nanotubes Composites. *J Nanostruct.* 2016; 6 (4): 278-284.
11. Jalajjerdi R, F. Gholamian F, Shafie H, Moraveji A, Ghanbari D, Thermal and Magnetic Characteristics of Cellulose Acetate- $Fe_3O_4$ . *J Nanostruct.* 2011; 1 (2): 105-109.
12. Horikoshi S, Serpone N. *Microwaves in nanoparticle synthesis: fundamentals and applications.* John Wiley & Sons. 2013.
13. Shinohara N. *Power without wires.* IEEE Microwave MPdazine, 2011; 12: S64-S73.
14. Tompsett G A, Conner W.C, Yngvesson K S. Microwave synthesis of nanoporous materials. *ChemPhysChem*, 2006; 7: 296-319.
15. Nabiyouni G, Ghanbari D, A. Yousofnejad A, Seraj M, Mirdamadian Z, Microwave-Assisted Synthesis of  $CuFe_2O_4$  Nanoparticles and Starch-Based Magnetic Nanocomposites. *J Nanostruct.* 2013; 3 (2): 155-160.
16. Ghanbari D, Salavati-Niasari M. Synthesis of urchin-like  $CdS$ - $Fe_3O_4$  nanocomposite and its application in flame retardancy of magnetic cellulose acetate. *J Ind Eng Chem.* 2015; 24: 284-292.
17. Ghanbari D, Salavati-Niasari M, Ghasemi-Kooch M. In situ and ex situ synthesis of poly (vinyl alcohol)- $Fe_3O_4$  nanocomposite flame retardants. *Particuology*, 2016; 26: 87-94.